2011 50th IEEE Conference on Decision and Control and
European Control Conference (CDC-ECC)
Orlando, FL, USA, December 12-15, 2011

Tracking an Unknown Two-Frequency Reference Using a Frequency Estimator-Based Servocompensator

Alex Esbrook, Xiaobo Tan, and Hassan K. Khalil

Abstract— **In this work, we address the tracking problem for an unknown reference comprised of two sinusoids. We propose an adaptive servocompensator based on a pair of frequency estimators. Slow adaptation is used to create three time scales within the closed-loop system, corresponding to the controller and plant dynamics, fast frequency estimate, and slow frequency estimate. Stability of the boundary-layer system, comprised of the servocompensator and plant dynamics, is achieved with a stabilizing controller. Novel nonlinear analysis is then performed on the average system to show global asymptotic stability. The algorithm's performance is verified by experiments conducted on a commercial nanopositioner, and its performance is shown to be comparable to that of iterative learning control.**

I. Introduction

Control of smart materials and other systems with hysteresis has seen much attention over the past few years [1]–[4]. In particular, piezoelectric-actuated systems have received a great deal of attention in the literature due to their wide use in nanopositioning systems [5], such as Scanning Probe Microscopy (SPM) [6]. An interesting approach to the control of such systems exploits (internal model-based) servocompensators [7], due to their performance at high frequency and ability to attenuate the hysteresis [8].

Internal model-based regulators [9], [10] have been the subject of ongoing research for the past several decades. Of particular note are adaptive internal model controllers [11]–[14], which can adapt their internal models to compensate for unknown reference signals or disturbances. Despite their merit, these adaptive servocompensators can require large numbers of adapted variables to compensate for harmonics generated by hysteresis, and can struggle to adapt these parameters when the harmonics are small. To overcome these problems, an adaptive internal model controller for linear systems that are subject to harmonic disturbances was proposed in [15]. This controller utilizes frequency estimation coupled with slow adaptation to create an adaptive servocompensator. The structure of the frequency estimator-based adaptive servocompensator allows for compensation of harmonics of the reference, without needing to adapt any parameters other than those associated with the internal model of the reference signal. An important example of such a case is when a pure sinusoidal reference is applied to systems involving a nonlinear operator such as hysteresis.

In this paper, we design a multiple-frequency estimation scheme combined with an internal model controller. Such a controller is motivated by cases where the reference signal is a sum of sinusoids of unknown frequencies. Since the adaptation scheme is based on frequency estimator and servocompensator, harmonics of the reference signals generated by nonlinear operators in the system can be compensated by expanding the internal model controller, without the need for additional adaptation variables, as done in [15]. While the analysis presented in this paper deals with the case where the reference is comprised of two different sinusoids, the method can be easily extended to the case of a sinusoidal reference and a sinusoidal matched disturbance of distinct frequencies. We demonstrate the global stability of the algorithm through rigorous analysis of the closed-loop system. The method is then tested experimentally on a commercial nanopositioning stage, and its performance is compared to iterative learning control [16].

The basic framework of the controller is similar to that of [15]. However the analysis is much more involved because of the increased number of frequencies to be estimated. We use slow adaptation and singular perturbation to split the system's dynamics into three timescales, for the dynamics of the controller and plant, then the (relatively) fast adaptation variable θ_1, and finally the slower adaptation variable θ_2, respectively. The analysis of the average system is conducted in two steps. First, we show that starting from any initial condition, the adaptation variable $\theta = [\theta_1, \theta_2]$ enters an arbitrarily small set Π around the point (ω_1, ω_2), where ω_1 and ω_2 are the frequencies to be estimated. We then show that a sufficiently small set Δ around the point (ω_1, ω_2) is positively invariant, and trajectories in this set converge to an equilibrium at (ω_1, ω_2). Since the size of Π can be chosen independently of the set Δ, we can always find a sufficiently small Π such that $\Pi \subset \Delta$, and subsequently we can conclude the asymptotic stability of the average system and ultimate boundedness of the closed-loop system.

The remainder of the paper is organized as follows. In Section II, we present the controller structure and discuss stability of the boundary-layer system. Section III presents the nonlinear analysis of the average system, and contains the main result of the paper. Experimental results and analysis are presented in Section IV, and concluding remarks are provided in Section V.

The work was supported by the National Science Foundation (CMMI 0824830).

A. Esbrook, X. Tan, and H. K. Khalil are with the Department of Electrical and Computer Engineering, Michigan State University, East Lansing, MI 48824. esbrooka@msu.edu (A. E.), xbtan@egr.msu.edu (X. T), khalil@egr.msu.edu (H. K.)

II. SYSTEM MODEL AND CONTROLLER DESIGN

The class of systems considered in this work consists of a linear system $G_p(s) = G_n(s)/G_d(s)$ with state x, subject to an unknown reference comprised of a pair of sinusoids. The control objective is to regulate the tracking error $e(t) = y_r(t) - y(t)$ to zero, where

$$\begin{aligned} \dot{x} =& Ax + Bu(t) \\ y(t) =& Cx \\ y_r(t) =& R_1 \sin(\omega_1 t + \psi_1) + R_2 \sin(\omega_2 t + \psi_2) \end{aligned} \tag{1}$$

and the variables comprising the reference trajectory y_r are unknown. It is assumed that the values of ω_1 and ω_2 lie within a known compact set Ω. The control signal $u(t)$ is formed using three components, illustrated in Fig. 1. First, a stabilizing controller $D(s)$ with state ξ will be designed to stabilize the closed-loop system in the absence of $C(s)$. This controller will be represented by the dynamic system,

$$\dot{\xi} = A_d \xi + B_d u_\xi \tag{2}$$

The second component will be an internal model-based controller (or servocompensator) $C(s)$ with state $\eta = [\eta_a, \eta_b]'$ where $'$ denotes the transpose, and is given by

$$\dot{\eta}_a = \mathbf{C}^*(\sigma_1)\eta_a + \mathbf{B}^* e(t) \tag{3}$$

$$\dot{\eta}_b = \mathbf{C}^*(\sigma_2)\eta_b + \mathbf{B}^* e(t) \tag{4}$$

where

$$\mathbf{C}^*(\sigma_i) = \begin{bmatrix} 0 & -\sigma_i \\ \sigma_i & 0 \end{bmatrix}, \mathbf{B}^* = \begin{bmatrix} 0 \\ 1 \end{bmatrix}$$

For later use, we also define

$$\bar{\mathbf{C}}^*(\sigma) = \begin{bmatrix} \mathbf{C}^*(\sigma_1) & 0 \\ 0 & \mathbf{C}^*(\sigma_2) \end{bmatrix}, \bar{\mathbf{B}}^* = \begin{bmatrix} \mathbf{B}^* \\ \mathbf{B}^* \end{bmatrix}$$

The servocompensator is dependent on the third element of the controller, the frequency estimator. This portion provides the frequency estimates $\sigma = [\sigma_1, \sigma_2]$ to the servocompensator. Note that the structure of $\mathbf{C}^*$ is such that if σ is known *a priori*, the system will have zero tracking error at the steady state [9]. The adaptation law, expanded from the design of that in [15], is given by

$$\dot{\sigma}_1 = -\gamma_1 \sigma_1^2 e(t) \frac{1}{s}[\eta_{a2}] \tag{5}$$

$$\dot{\sigma}_2 = -\gamma_2 \sigma_2^2 e(t) \frac{1}{s}[\eta_{b2}] \tag{6}$$

where η_{a2} and η_{b2} denote the second components of η_a and η_b, respectively. Projection is used to ensure that the estimate $\sigma \in \Omega_\sigma$, where $\Omega \subset \Omega_\sigma$. Throughout the paper, the notation $F(s)[g(t)]$ will denote filtering of the time-domain signal $g(t)$ by the transfer function $F(s)$. The interconnection of the servocompensator and the stabilizing controller is defined by

$$u_\xi = k_\eta(\sigma)\eta + D_c(\sigma)e(t) \tag{7}$$

and the applied control to the plant is given by

$$u(t) = C_d \xi + D_d(k_\eta(\sigma)\eta + D_c(\sigma)e(t)) \tag{8}$$

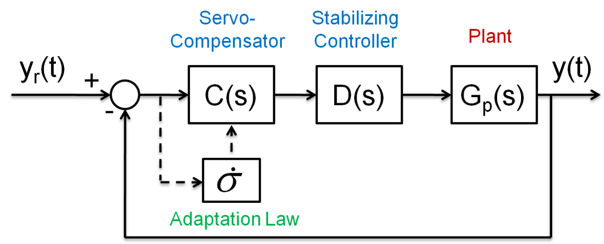

Fig. 1. Block Diagram of the closed-loop system.

In (7), k_η and $D_c(\sigma)$ are chosen so that $C(s)$ behaves like a notch filter. This is done so that the added servocompensator does not ruin the stability of the closed-loop system already ensured by the stabilizing controller $D(s)$, i.e. for $\sigma = (\sigma_1, \sigma_2)$,

$$C(s) = \frac{s^2 + 2\zeta_c\sigma_1 s + \sigma_1^2}{s^2 + \sigma_1^2} \frac{s^2 + 2\zeta\sigma_2 s + \sigma_2^2}{s^2 + \sigma_2^2} \tag{9}$$

ζ and ζ_c can be chosen to be identical, however we make the distinction here for use in our analysis of the average system.

A. Stability of the Boundary Layer System

Equations (1) to (8) form a complete description of the closed-loop system. We now define the first boundary-layer system, defined by setting $\gamma_1 = \gamma_2 = 0$ in (5) and (6). This freezes the value of σ at σ_{bl}. Denoting the state variables of the boundary-layer system as $\chi_{bl} = [x_{bl}', \eta_{bl}', \xi_{bl}']'$, the closed-loop boundary-layer system is then,

$$\begin{aligned} \dot{\chi}_{bl} =& F_{bl}(\chi_{bl}, \sigma_{bl}, t) \\ =& \begin{bmatrix} A - BD_dD_c(\sigma_{bl})C & BD_dk_\eta(\sigma_{bl}) & BC_d \\ -\bar{\mathbf{B}}^*C & \bar{\mathbf{C}}^*(\sigma_{bl}) & 0 \\ -B_dD_c(\sigma_{bl})C & B_dk_\eta(\sigma_{bl}) & A_d \end{bmatrix} \chi_{bl} \\ &+ \begin{bmatrix} BD_dD_c(\sigma_{bl})y_r(t) \\ \bar{\mathbf{B}}^* y_r(t) \\ B_dD_c(\sigma_{bl})y_r(t) \end{bmatrix} \end{aligned} \tag{10}$$

This system is nearly identical to the boundary layer system considered in [15]. Since we have chosen $k_\eta(\sigma_{bl})$ and $D_c(\sigma_{bl})$ such that $C(s)$ behaves like a notch filter, we can then design the stabilizing compensator $D(s)$ to stabilize this system over all $\sigma_{bl} \in \Omega_\sigma$. We will denote the steady state solution of χ_{bl} under a frozen σ_{bl} as $\bar{\chi}(\sigma_{bl})$.

III. AVERAGE SYSTEM ANALYSIS

After establishing the stability of the boundary-layer system, we can now move to the computation and analysis of the average system. The average system with state $\theta = [\sigma_{1av}, \sigma_{2av}]'$ is formed as follows:

$$\begin{aligned} \dot{\theta} =& F_{av}(\bar{\chi}_{bl}(\theta), \theta) \\ =& \begin{bmatrix} -\lim_{T\to\infty} \frac{\gamma_1}{T} \int_0^T \sigma_{1av}^2 e(t) \frac{1}{s}[\eta_{a2}]\, dt \\ -\lim_{T\to\infty} \frac{\gamma_2}{T} \int_0^T \sigma_{2av}^2 e(t) \frac{1}{s}[\eta_{b2}]\, dt \end{bmatrix} \end{aligned} \tag{11}$$

To simplify the notation, we will write

$$\theta = [\theta_1, \theta_2]' \triangleq [\sigma_{1av}, \sigma_{2av}]'$$

The evaluation of (11) is shown in equations (12) and (13) on the next page.

We will assume $1 >> \gamma_1 >> \gamma_2$, which will create a time scale separation between the dynamics of θ_1 and θ_2. Our task is to show the stability of the coupled average systems. Looking at equations (12) and (13), it is tempting to simply apply Lyapunov analysis in order to determine stability without requiring multiple time scales in the adaptation. However, this analysis breaks down fairly quickly. Consider the Lyapunov function candidate

$$V(\theta) = \frac{(\theta_1 - \omega_1)^2}{2} + \frac{(\theta_2 - \omega_2)^2}{2} \triangleq \frac{\tilde{\theta}_1^2}{2} + \frac{\tilde{\theta}_2^2}{2} \quad (14)$$

Taking a derivative of $V(t)$ along the solutions of (12) and (13), we quickly run into the following issue; where do the signs of $\dot{\theta}_1$ and $\dot{\theta}_2$ change? It is possible to find the answer by computation of the resulting terms, but this will imply that the stability of the plant depends on a complicated relationship between plant parameters as well as the unknown frequencies. Therefore, instead of proceeding with a strictly Lyapunov-based analysis, we exploit the multi-time-scale nature of the adaptation to show that θ_1 will converge to a point contained inside a particular collection of compact sets. Then, we can investigate the behavior of the θ_2 subsystem when θ_1 is within these sets, which allows us to argue that θ enters a neighborhood of the desired equilibrium point, on which it is possible to show that the derivative of (14) is negative definite. We will also require the following assumption, which is commonly used in singular perturbation and averaging theory [17].

Assumption 1: The dynamics of θ_1 have distinct real equilibria.

Following the singular perturbation theory outlined in [17], we will now show that the dynamics for θ_1 settle at a stable equilibrium point. Our first step is to check for the existence and locations of equilibrium points. We compute the denominator terms of (12) as $\bar{D}(\theta_1, \theta_2, \omega_1)$ and $\bar{D}(\theta_1, \theta_2, \omega_2)$ for the first and second fractions respectively. This is done by splitting up the transfer functions $G_d(j\omega_1)$ and $G_n(j\omega_1)$ into real and imaginary components. This expansion is included in equation (15) located on the next page.

As a shorthand, define for $i = 1, 2$,

$$\begin{aligned}
D_{1Re}(\omega_i) &\triangleq Re(G_p(j\omega_i))(\theta_2^2 - \omega_i^2)\\
D_{2Re}(\omega_i) &\triangleq Re(G_n(j\omega_i)D(j\omega_i)(\theta_2^2 + 2\zeta\omega_i\theta_2 j - \omega_i^2))\\
D_{1Im}(\omega_i) &\triangleq Im(G_p(j\omega_i))(\theta_2^2 - \omega_i^2)\\
D_{2Im}(\omega_i) &\triangleq Im(G_n(j\omega_i)D(j\omega_i)(\theta_2^2 + 2\zeta\omega_i\theta_2 j - \omega_i^2))\\
D_{mag}(\omega_i) &\triangleq D_{1Re}^2(j\omega_i) + D_{2Re}^2(j\omega_i)\\
&\quad + D_{2Im}^2(j\omega_i) + D_{2Im}^2(j\omega_i)
\end{aligned}$$

We can then use the above definitions to write $\bar{D}$ in (15) as

$$\begin{aligned}
\bar{D}(\theta_1, \theta_2, \omega_1) =& [(D_{1Re} + D_{2Re})(\theta_1^2 - \omega_1^2) - D_{2Im}2\zeta\omega_1\theta_1]^2\\
&+ [(D_{1Im} + D_{2Im})(\theta_1^2 - \omega_1^2) + D_{2Re}2\zeta\omega_1\theta_1]^2
\end{aligned} \quad (16)$$

The above expression implies that the shorthand terms have been evaluated at ω_1. Next, we define

$$\begin{aligned}
c_1 =& \gamma_1\theta_1^2|\theta_2^2 - \omega_1^2|^2|G_d(j\omega_1)^2|\\
c_2 =& \gamma_1\theta_1^2|\theta_2^2 - \omega_2^2|^2|G_d(j\omega_2)^2|
\end{aligned}$$

Setting $\dot{\theta}_1$ equal to zero, and multiplying both sides of (12) by the denominators, we arrive at the equation

$$0 = -c_2\bar{D}(\theta_1, \theta_2, \omega_1)(\theta_1^2 - \omega_2^2) - c_1\bar{D}(\theta_1, \theta_2, \omega_2)(\theta_1^2 - \omega_1^2) \quad (17)$$

Canceling the θ_1^2 terms, we can expand this expression into a 6th-order polynomial in θ_1 with the form

$$0 = a_6\theta_1^6 + a_5\theta_1^5 + a_4\theta_1^4 + a_3\theta_1^3 + a_2\theta_1^2 + a_1\theta_1^1 + a_0 \quad (18)$$

The roots of this polynomial correspond to the equilibrium points of the θ_1 dynamics. We do not need to use the exact form of this equation (indeed it is too complex to be of much use); however, we will need to make use of the fact that the notch filter parameter ζ_c will appear linearly and quadratically as a parameter of the coefficients of this polynomial, which can be seen from the form of (15). Letting the notch filter parameter ζ_c in $\bar{D}(\cdot)$ equal zero, we can evaluate the aforementioned polynomial as

$$\begin{aligned}
0 =& -c_1 D_{mag}(\omega_2)(\theta_1^2 - \omega_1^2)|\theta_1^2 - \omega_2^2|^2\\
&- c_2 D_{mag}(\omega_1)(\theta_1^2 - \omega_2^2)|\theta_1^2 - \omega_1^2)|^2
\end{aligned} \quad (19)$$

This equation possesses positive equilibrium points at ω_1, ω_2 and a third between ω_1 and ω_2. We can now use the continuity of polynomial functions in their parameters to show that the equilibriums of the real system, given by the roots of (18), must be near those of the equation (19). In particular, if r_i is the ith root of (18) and r_i' is the ith root of (19), for any $\varepsilon_1 > 0$, there exists a δ such that when $\zeta < \delta$, $|r_i - r_i'| < \varepsilon_1$ [18]. Furthermore, since θ_2 is bounded, the effect of θ_2 on the difference between (18) and (19) is bounded, therefore ε_1 can be chosen independently of θ_2.

Remark 1: From (12) we know that $\dot{\theta}_1$ is positive when $\theta_1 < \omega_1$ and negative when $\theta_1 > \omega_2$. By the same logic, we can see that θ enters the set $[\omega_1, \omega_2] \times [\omega_1, \omega_2]$ from any bounded initial condition.

According to Remark 1, any root of the θ_1 dynamics must be within the closed interval $[\omega_1, \omega_2]$. From [18], we know that for a sufficiently small ζ_c, (18) possess three roots within the interval $[\omega_1, \omega_2]$. In addition, there must exist roots within an ε_1 interval of both ω_1 and ω_2. From Assumption 1, we know that there are either one or three real roots within this range of interest. Together with Remark 1, if there are three equilibrium points, the first and third must always be asymptotically stable and within an ε_1-interval of ω_1 and ω_2 respectively, with an unstable equilibrium point between them. If there is one real root and one complex pair, we again

$$\dot{\theta}_1 = -\frac{\gamma_1\theta_1^2|\theta_2^2-\omega_1^2|^2|G_d(j\omega_1)^2|(\theta_1^2-\omega_1^2)}{|G_d(j\omega_1)(\theta_1^2-\omega_1^2)(\theta_2^2-\omega_1^2)+D(j\omega_1)G_n(j\omega_1)(\theta_1^2+2\zeta_c\omega_1\theta_1 j-\omega_1^2)(\theta_2^2+2\zeta\omega_1\theta_2 j-\omega_1^2)|^2}$$
$$-\frac{\gamma_1\theta_1^2|\theta_2^2-\omega_2^2|^2|G_d(j\omega_2)^2|(\theta_1^2-\omega_2^2)}{|G_d(j\omega_2)(\theta_1^2-\omega_2^2)(\theta_2^2-\omega_2^2)+D(j\omega_2)G_n(j\omega_2)(\theta_1^2+2\zeta_c\omega_2\theta_1 j-\omega_2^2)(\theta_2^2+2\zeta\omega_2\theta_2 j-\omega_2^2)|^2} \quad (12)$$

$$\dot{\theta}_2 = -\frac{\gamma_2\theta_2^2|\theta_1^2-\omega_1^2|^2|G_d(j\omega_1)^2|(\theta_2^2-\omega_1^2)}{|G_d(j\omega_1)(\theta_2^2-\omega_1^2)(\theta_1^2-\omega_1^2)+D(j\omega_1)G_n(j\omega_1)(\theta_2^2+2\zeta\omega_1\theta_1 j-\omega_1^2)(\theta_1^2+2\zeta_c\omega_1\theta_1 j-\omega_1^2)|^2}$$
$$-\frac{\gamma_2\theta_2^2|\theta_1^2-\omega_2^2|^2|G_d(j\omega_2)^2|(\theta_2^2-\omega_2^2)}{|G_d(j\omega_2)(\theta_2^2-\omega_2^2)(\theta_1^2-\omega_2^2)+D(j\omega_2)G_n(j\omega_2)(\theta_2^2+2\zeta\omega_2\theta_2 j-\omega_2^2)(\theta_1^2+2\zeta_c\omega_2\theta_1 j-\omega_2^2)|^2} \quad (13)$$

$$\begin{aligned}\bar{D}(\theta_1,\theta_2,\omega_1) =& |G_d(j\omega_1)(\theta_1^2-\omega_1^2)(\theta_2^2-\omega_1^2)+D(j\omega_1)G_n(j\omega_1)(\theta_1^2+2\zeta_c\omega_1\theta_1 j-\omega_1^2)(\theta_2^2+2\zeta\omega_1\theta_2 j-\omega_1^2)|^2\\ =& [Re(G_d(j\omega_1))(\theta_1^2-\omega_1^2)(\theta_2^2-\omega_1^2)+Re(G_n(j\omega_1)(\theta_2^2+2\zeta\omega_1\theta_2 j-\omega_1^2))(\theta_1^2-\omega_1^2)\\ &-Im(G_n(j\omega_1)D(j\omega_1)(\theta_2^2+2\zeta\omega_1\theta_2 j-\omega_1^2))2\zeta_c\omega_1\theta_1]^2\\ &+[Im(G_d(j\omega_1)(\theta_1^2-\omega_1^2)(\theta_2^2-\omega_1^2)+Im(G_n(j\omega_1)(\theta_2^2+2\zeta\omega_1\theta_2 j-\omega_1^2))(\theta_1^2-\omega_1^2)\\ &+Re(G_n(j\omega_1)D(j\omega_1)(\theta_2^2+2\zeta\omega_1\theta_2 j-\omega_1^2))2\zeta_c\omega_1\theta_1]^2\end{aligned} \quad (15)$$

know from Remark 1 that the root is asymptotically stable. In addition, for a sufficiently small ζ_c, $|\omega_1-\omega_2|>2\varepsilon_1$, therefore since two roots must always be within ε_1 intervals of ω_1 and ω_2, the roots near ω_1 and ω_2 cannot both be complex. Thus, when there is one real root, it is within an ε_1-interval of either ω_1 or ω_2.

We can then use this result to show that θ_2 will always converge to a neighborhood of either ω_1 or ω_2. For clarity of presentation, we will now make the following two assumptions; first, that the initial condition of θ is such that θ_1 converges to near ω_1 and θ_2 converges to near ω_2, and second that $\omega_1<\omega_2$. We will remark on the first of these assumptions following the statement of Theorem 1. The second assumption can clearly be made without loss of generality. Returning to the equation for θ_2, we can now treat the term related to $|\theta_1^2-\omega_1^2|^2$ as being of order $O(\varepsilon_1^2)$. This reduces the θ_2 dynamics to those of a single-frequency system with a small perturbation, a case that can be analyzed by extending the techniques of [15].

If the initial condition of θ_2 is such that it must pass through ω_1 to reach ω_2 (i.e. $\theta_2(0)<\omega_1$), we require additional analysis. From (12), note that as θ_2 approaches ω_1 (say ε_3-close, i.e. $\theta_2\in[\omega_1-\varepsilon_3,\omega_1+\varepsilon_3]$), the term $|\theta_2^2-\omega_1^2|^2$ is of order $O(\varepsilon_3^2)$. Furthermore, note that $|\theta_2^2-\omega_2^2|^2$ is bounded in an $O(\varepsilon_3^2)$-neighborhood of $|\omega_1^2-\omega_2^2|^2$ for θ_2 ε_3-close to ω_1. Next, for all $\omega_c\in[\omega_1,\omega_2]$ and bounded θ, we can find positive constants β_3 and β_4, and β_5 such that

$$\beta_3 \le \bar{D}(\theta_1,\theta_2,w_c) \le \beta_4+\beta_5\zeta_c \quad (20)$$

where the existence of β_3 is guaranteed from the stability properties of the boundary layer system. Therefore, if θ_2 is ε_3-close to ω_1, we can find positive constants ρ_1 and ρ_2 to form the bound

$$\dot{\theta}_1 \ge -\frac{\rho_1}{\beta_3^2}\varepsilon_3^2+\frac{\rho_2}{\beta_4+\beta_5\zeta_c} \quad (21)$$

Also recall that from our stability discussions, we have imposed the restriction $\zeta_c << 1$. Thus, for a sufficiently small ε_3, if $\theta_2\in[\omega_1-\varepsilon_3,\omega_1+\varepsilon_3]$, $\dot{\theta}_1$ is positive for $\theta_1\in(0,\omega_1+\varepsilon_4)$, for any $\zeta_c<<1$, where ε_4 grows uniformly with ε_3. Since ε_3 (and therefore ε_4) can be chosen independently of ζ_c, we can select $\varepsilon_3>\varepsilon_1$, implying there is no real root in the interval $\theta_1\in[\omega_1,\omega_1+\varepsilon_1]$. However, from (19) and [18], there must be a root of the θ_1 dynamics r_1 satisfying $|r_1-\omega_1|<\varepsilon_1$; thus the root r_1 is complex, which implies that the θ_1 dynamics posses an asymptotically stable equilibrium point within an ε_1 region of ω_2. In effect, the condition of both θ_1 and θ_2 being close to ω_1 causes the equilibrium point of the θ_1 dynamics near ω_1 to disappear; i.e., as θ_2 approaches ω_1, it causes a bifurcation within the system, eliminating the equilibrium point at which θ_1 had settled at, and forcing θ_1 to the region near ω_1. Once this transition occurs, the system has essentially returned to the first case described above. Therefore, we have established that θ enters a set Π, where either

$$\Pi \triangleq \{\theta:\theta_1\in[\omega_1,\omega_1+\varepsilon_1],\theta_2\in[\omega_2-\varepsilon_2,\omega_2]\}$$

or

$$\Pi \triangleq \{\theta:\theta_1\in[\omega_2-\varepsilon_1,\omega_2],\theta_2\in[\omega_1,\omega_1+\varepsilon_2]\}$$

Should θ_1 converges to an equilibrium point near θ_2, or θ_2 must pass through ω_1, convergence to one of the two options for Π can be shown following the same logic as above.

We have now essentially proven ultimate boundedness of the frequency estimates. However, we can conclude asymptotic stability of the combined average dynamics (12) and (13) by investigating the behavior of the combined average dynamics in a small neighborhood of (ω_1,ω_2). Consider the set $\Delta\triangleq\{|\tilde{\theta}_1|<\varepsilon_c,|\tilde{\theta}_2|<\varepsilon_c\}$. Next, we consider the Lyapunov function candidate (14). Taking the time derivative yields

$$\dot{V} = \tilde{\theta}_1 \dot{\theta}_1 + \tilde{\theta}_2 \dot{\theta}_2 \tag{22}$$

We seek to find an ε_c such that $\dot{V}$ is negative definite. Assuming that the system is currently within the set Δ, we substitute $\theta_1 = \omega_1 + \tilde{\theta}_1$ and $\theta_2 = \omega_2 + \tilde{\theta}_2$ where $\tilde{\theta}_1, \tilde{\theta}_2 \in [-\varepsilon_c, \varepsilon_c]$. Using these substitutions together with (12)-(13), we can then bound $\dot{V}$ by

$$\begin{aligned}\dot{V} \leq & \frac{-\tilde{\theta}_1^2}{|D(jw_1)|^2}[-|2w_1+\varepsilon_c|^2|\gamma_2 G_d(j\omega_2)^2||(w_2-w_1+\varepsilon_c)\varepsilon_c \\ & +|w_1^2-w_2^2+2w_1\varepsilon_c+\varepsilon_c^2|^2||\gamma_1 G_d(j\omega_1)^2|] \\ & +\frac{-\tilde{\theta}_2^2}{|D(jw_2)|^2}[|2w_2+\varepsilon_c|^2||\gamma_1 G_d(j\omega_2)^2||(w_1-w_2-\varepsilon_c)\varepsilon_c \\ & +|w_2^2-w_1^2-2w_2\varepsilon_c+\varepsilon_c^2|^2||\gamma_2 G_d(j\omega_1)^2|]\end{aligned} \tag{23}$$

Clearly, a sufficiently small ε_c guarantees that $\dot{V}$ is negative definite within the set Δ. Since the terms in the brackets of (23) are independent of ζ_c, the value of ε_c (and therefore the size of the set Δ) can be made independently of ζ_c, and therefore independent of ε_1 and ε_2. Therefore we conclude that trajectories starting in the set Δ asymptotically converge to the equilibrium point $\theta = [\omega_1, \omega_2]$. Since the choice of ε_c was made independent of the choice of ζ_c, we can always find a ζ_c such that the trajectory of θ enters Δ. We make the result formal with the following theorem.

Theorem 1: Let assumption 1 hold. Let ζ in (9) be such that $\Pi \subset int(\Delta)$. Then θ asymptotically converges to $[\omega_1, \omega_2]$.

With this result, we can then apply the averaging framework of [19] to conclude stability of the closed loop system (χ, σ) and convergence of the tracking error to zero.

IV. Experimental Results

We now verify the proposed method experimentally on a commercial nanopositioner. The modeling procedure used was detailed in [8], and is based on a modified Prandtl-Ishlinskii (PI) [20] hysteresis operator cascaded with linear dynamics. The adaptation gains used were 0.15 and 0.02 for the fast and slow estimates respectively. In order to mitigate the hysteresis, an inverse PI operator [20] is added to the controller. Stabilization of the system is facilitated by the following stabilizing controller,

$$D(s) = \frac{2.083 \times 10^7}{s^2 + 4900s + 1.225 \times 10^7} \tag{24}$$

We first test the steady-state performance of the proposed method, which we will refer to as an Adaptive Servocompensator (ASC), and compare its performance to that of Iterative Learning Control (ILC), a popular and effective control method used in nanopositioning research [16]. The reference signal used for this experiment is a sum of two sinusoids. The frequencies of the two sinusoids are determined in part by the constant W, which we use to determine the overall speed of the reference. For our first set of experiments, we use sinusoids of frequency $1.3W$ and $0.7W$, and two different values of W, $2\pi 10$ and $2\pi 100$. Initial conditions were $1.2W$ and $.6W$ for the slow and fast frequency estimators respectively. The error metric we will use is the mean tracking error, computed as the mean of $|e(t)|$ over one period of the reference.

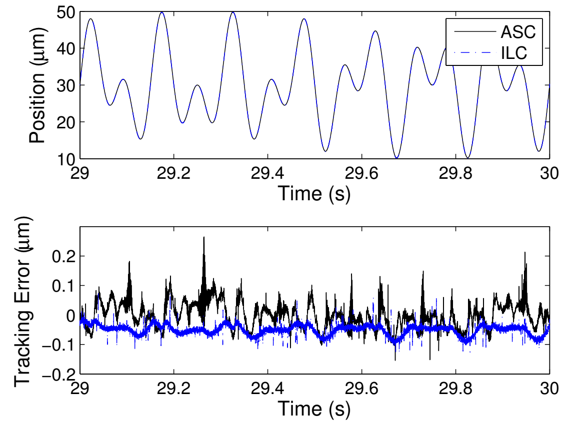

Fig. 2. Output and tracking error for $W = 2\pi 10$.

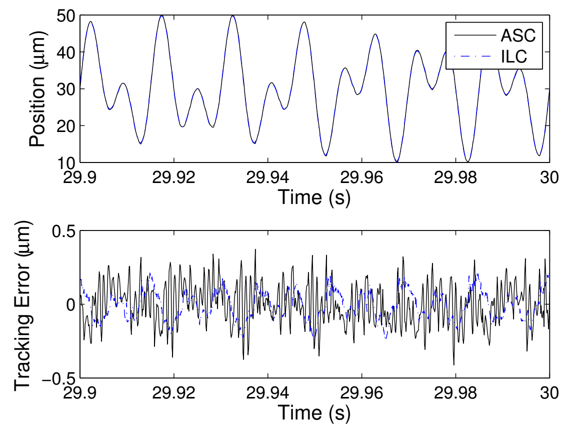

Fig. 3. Output and tracking error for $W = 2\pi 100$.

The results of these tests are shown in Fig. 2 and 3. For $W = 2\pi 10$, the methods provide very similar performance in terms of the error metric, which comes out to be 0.035 μm for the ASC and 0.034 μm for ILC. When the signal is accelerated to $W = 2\pi 100$, the difference between the two controllers opens up, with 0.0723 μm mean error for ILC and 0.1120 μm for the ASC. However, the nature of that error is very different. With the ASC, the tracking error is primarily comprised of the higher harmonics of the reference signal, while much of ILC's error comes from an offset in the signal.

We now analyse the adaptation performance. For this test, we will use a reference whose frequencies change at certain points in time. Again, the overall speed of the reference is tied to the constant $W = 2\pi 10$. The initial reference is $1.3W$ and $0.7W$. This changes to $1.3W$ and $0.5W$ at 20s, then $1.2W$ and $0.6W$ at 40s. Fig. 4 shows the tracking error and parameter values when this reference trajectory is used.

We first notice the difference in convergence times on the fast and slow estimates. After the adaptation is turned on after at 2s, we can see that the fast estimate converges around 7s, while the slow variable takes until just before the reference switches at 20s. With the second reference trajectory ($1.3W$ and $0.5W$), we observe that the slow estimate moves away slightly from the desired value, even though it started at $1.3W$. This behavior is what would be expected from the analysis of the system. Recall that we originally show that for a given value of the slow variable θ_2, the fast variable θ_1 will settle to a small neighborhood of the desired frequency due to continuity of the equilibrium locations with ζ_c. This same line of thinking can be applied to the slow variable θ_2 when θ_1 is far away from either frequency.

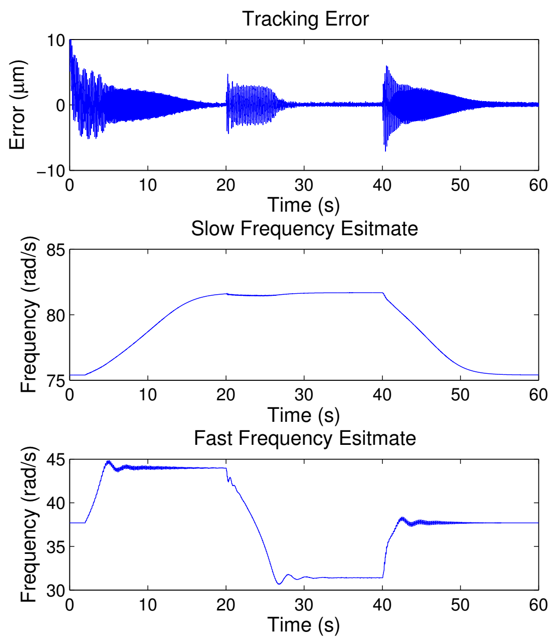

Fig. 4. Results for a changing reference signal $W = 2\pi 10$. Adaptation is turned on at 2s. Reference frequencies start as $1.3W, 0.7W$, then at 15s switch to $1.3W, 0.5W$, then at 30s switch to $1.2W, 0.6W$.

V. Conclusion

We have extended the design of the frequency-estimator based adaptive servocompensator proposed in [15] to the case where the reference signal is comprised of a pair of unknown sinusoids. Rigorous analysis of the resulting closed-loop system has been conducted under a novel combination of averaging and nonlinear analysis tools. We have verified the effectiveness of the proposed method experimentally. In addition, we have been able to observe nonlinear behaviors expected from the analysis of the closed-loop system.

Experimental and simulation results seem to imply that the restriction of multiple time scale adaptation, i.e. $\gamma_1 >> \gamma_2$, may be unnecessary. Analysis of such a system will be considered in our future work. Encouraged by the success of implementing the proposed algorithm on a plant significantly more complex than that considered in the analysis, we plan to advance the systems considered in the analysis to include linear dynamics preceded by hysteresis. Efforts to generalize the proposed method to an n-frequency case, or when there are unknown sinusoidal matched disturbances are underway. In addition, we plan on expanding the internal model controller to compensate for harmonics of the reference signal.

References

[1] A. Cavallo, C. Natale, S. Pirozzi, and C. Visone, "Effects of hysteresis compensation in feedback control systems," *IEEE Transactions on Magnetics*, vol. 39, no. 3, pp. 1389 – 1392, 2003.

[2] R. Iyer, X. Tan, and P. Krishnaprasad, "Approximate inversion of the preisach hysteresis operator with application to control of smart actuators," *IEEE Transactions on Automatic Control*, vol. 50, no. 6, pp. 798 – 810, 2005.

[3] X. Tan and J. S. Baras, "Modeling and control of hysteresis in magnetostrictive actuators," *Automatica*, vol. 40, no. 9, pp. 1469–1480, 2004.

[4] X. Tan and R. Iyer, "Modeling and control of hysteresis: Introduction to the special section," *IEEE Control Systems Magazine*, vol. 29, no. 1, pp. 26–29, 2009.

[5] S. Devasia, E. Eleftheriou, and S. O. R. Moheimani, "A survey of control issues in nanopositioning," *IEEE Transactions on Control Systems Technology*, vol. 15, pp. 802–823, 2007.

[6] D. Croft, G. Shed, and S. Devasia, "Creep, hysteresis, and vibration compensation for piezoactuators: Atomic force microscopy application," *Journal of Dynamic Systems, Measurement, and Control*, vol. 123, no. 1, pp. 35–43, 2001.

[7] Y. Shan and K. K. Leang, "Repetitive control with prandtl-ishlinskii hysteresis inverse for piezo-based nanopositioning," in *Proceedings of the 2009 American Control Conference*, 2009, 301-306.

[8] A. Esbrook, M. Guibord, X. Tan, and H. K. Khalil, "Control of systems with hysteresis via servocompensation and its application to nanopositioning," in *Proceedings of the 2010 American Control Conference*, 2010, pp. 6531–6536.

[9] E. J. Davison, "The output control of linear time-invariant multivariable systems with unmeasurable arbitrary disturbances," *IEEE Transactions on Automatic Control*, vol. 17, no. 5, pp. 621–630, 1972.

[10] B. Francis and W. Wonham, "The internal model principle for linear multivariable regulators," *Applied Mathematics and Optimization*, vol. 2, pp. 170–194, 1975.

[11] H. Elliott and G. C. Goodwin, "Adaptive implementation of the internal model principle," in *Proceedings of the 23rd IEEE Conference on Decision and Control*, 1984, pp. 1292 – 1297.

[12] A. Isidori and C. I. Byrnes, "Output regulation of nonlinear systems," *IEEE Transactions on Automatic Control*, vol. 35, no. 2, pp. 131–140, 1990.

[13] V. Nikiforov, "Adaptive nonlinear tracking with complete compensation of unknown disturbances," *European Journal of Control*, vol. 4, pp. 132–139, 1998.

[14] A. Serrani, A. Isidori, and L. Marconi, "Semiglobal nonlinear output regulation with adaptive internal model," *IEEE Transactions on Automatic Control*, vol. 46, no. 8, pp. 1178–1194, 2001.

[15] A. Esbrook, X. Tan, and H. K. Khalil, "Regulation under disturbances with multiple harmonics of unknown frequency," in *Proceedings of the 2011 American Control Conference*, 2011, to appear.

[16] Y. Wu and Q. Zou, "Iterative control approach to compensate for both the hysteresis and the dynamics effects of piezo actuators," *IEEE Transactions on Control Systems Technology*, vol. 15, no. 5, pp. 936–944, 2007.

[17] H. K. Khalil, *Nonlinear Systems*, 3rd ed. Upper Saddle River, NJ: Prentice Hall, 2002.

[18] F. Cucker and A. G. Corbalan, "An alternate proof of the continuity of the roots of a polynomial," *The American Mathematical Monthly*, vol. 96, no. 4, pp. 342–345, 1989.

[19] S. Sastry and M. Bodson, *Adaptive control : stability, convergence, and robustness*. Prentice Hall, Englewood Cliffs, N.J. :, 1989.

[20] K. Kuhnen, "Modeling, identification and compensation of complex hysteretic nonlinearities - a modified Prandtl-Ishlinskii approach," *European Journal of Control*, vol. 9, no. 4, pp. 407–418, 2003.